Interfacial Studies in CTBN-Modified Epoxies

R. BAGHERI and R. A. PEARSON*

Polymer Interfaces Center and Department of Materials Science and Engineering, Lehigh University, Bethlehem, Pennsylvania 18015

SYNOPSIS

Rubber particle cavitation and concomitant shear deformation of the matrix is known to be a major source of toughening in rubber-modified epoxies. The role of the rubber–matrix interface in this toughening mechanism, however, is not well studied. It has been claimed by Chen and Jan [Polym. Eng. Sci., 31, 577 (1991)] that introduction of a ductile interphase around the rubbery phase enhances plastic dilation of particles and thus contributes to fracture energy of modified blend. In spite of this promising development in rubber toughening, very few studies on the use of ductile interfaces to improve the fracture resistance of rubber-modified polymers have been initiated. The objective of this investigation is to examine the role of ductility of interface on the fracture toughness of rubber-modified epoxies. Both ductile and rigid interphases are incorporated around CTBN particles in a DGEBA epoxy matrix via end-capping of rubber with epoxy monomers different from that of the matrix. The results of this investigation suggest that introduction of a ductile interphase may indeed further improve the crack growth resistance of material under certain test conditions. In contrast, introduction of the rigid interphase, in the system studied, promoted interfacial debonding and plastic dilation but did not alter the mechanical performance of the rubber-modified blend. © 1995 John Wiley & Sons, Inc.

INTRODUCTION

Rubber modification, i.e., addition of a rubbery particulate phase to a glassy polymer matrix, has been found to be a very successful approach for improving the toughness of brittle epoxy resin.[1-8] Studying the sources of this improvement in crack growth resistance has been the subject of many investigations over the past two decades. It is known that plastic deformation of the matrix is responsible for the toughening effect in rubber-modified epoxies.[7-11] The plastic deformation, which is induced by rubber particles, can be divided into (1) localized shear yielding, or shear banding, usually between the neighboring particles and (2) plastic void growth, which is initiated by cavitation or debonding of rubber particles.[12] While some researchers[10,11] focused on shear banding as the dominant toughening mechanism, Huang and Kinloch[13] raised the importance of plastic void growth as the second energy dissipating mechanism in these systems.

Kozii and Rozenberg[14] thoroughly reviewed the literature on rubber-modified epoxies and claimed that while the interface in rubber-modified thermosets may play an important role in toughening, as it does in many composite systems, very few investigations have touched this matter. Most of the work performed to date is limited to the problem of adhesion at interface.[15-17] It has been shown experimentally that when the second phase consists of micron-size rubber particles, the interfacial bonding has only a modest effect on the fracture properties of the blend.[17] This finding would be anticipated if one considers that rubber particles cavitate and thus act similarly to that of holes. Therefore, their function should not alter by changing their degree of adhesion to the matrix. Indeed our study on epoxy modified by hollow plastic particles[18] revealed that there is little difference between the use of preformed holes and conventional rubber modifiers in toughening of a diglycidyl ether of bisphenol A (DGEBA) epoxy (at low volume fractions).

* To whom correspondence should be addressed.

Journal of Applied Polymer Science, Vol. 58, 427–437 (1995)
 CCC 0021-8995/95/020427-11

The role of interface in rubber-modified epoxies can be viewed from another perspective, that is, the ductility of the interfacial zone. In other words, one may look at the problem of interface in a case that an interphase exists between the rubber particle and the matrix (Fig. 1). This interphase may have different properties from the matrix and, therefore, might influence the toughening mechanism(s). Matonis[19] modeled the influence of a ductile shell on the stress distribution around a very soft particle located in an infinite matrix which was subjected to uniaxial tension. This elastic stress analysis showed that introduction of such an interphase hardly disrupts the stress field associated with the pure two-phase material. In contrast, Chen and Jan[20] took an experimental approach in which a ductile interphase was introduced around carboxyl terminated butadiene acrylonitrile copolymers (CTBN) rubber particles in an epoxy matrix through end-capping of the liquid rubber with the flexible epoxy chains. The resulting interphase is a diffuse zone which is rich in end-capping elements. This interphase is formed around the CTBN particles during the crosslinking of the matrix when the rubbery phase precipitates out. Chen and Jan[20] claimed that the incorporation of such a ductile interphase improves fracture energy of the blend dramatically.

The purpose of this research is to further elucidate the role of deformability of the interfacial zone in rubber-modified epoxies. The approach taken investigates both ductile and stiff interphases in CTBN-modified epoxies. Interphases are introduced via end-capping the CTBN oligomers by different epoxy monomers. The emphasis is placed on fractography and optical microscopy rather than synthesis and characterization of the interphase regions.

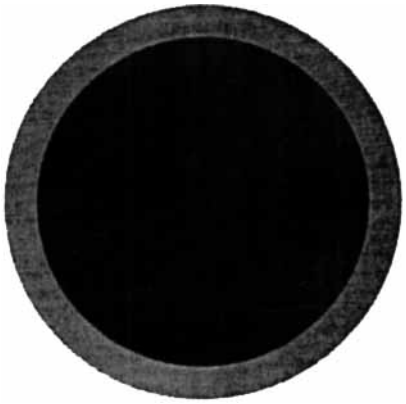

Figure 1 Schematic showing an interphase surrounding the rubber particle. Having different ductility from that of the matrix, this interphase may influence the deformation in the vicinity of the particle and thus affects the toughening mechanism.

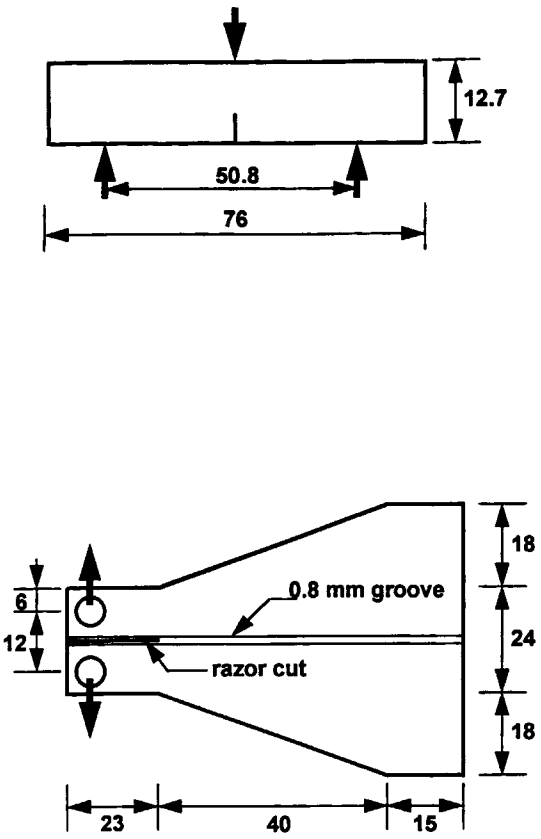

Figure 2 Schematic illustration of the SEN-3PB (top) and the TDCB (bottom) specimens used in this study. Dimensions are in millimeters.

EXPERIMENTAL

Materials

The epoxy system used in this investigation consisted of a solid DGEBA epoxy resin with an epoxy equivalent weight of about 530 g/eq cured with 4,4′-diamino-diphenyl sulphone (DDS). The DGEBA epoxide resin used in this study was DER 661 resin from the Dow Chemical Co. The rubber used was a carboxyl-terminated random copolymer of butadiene and acrylonitrile (Hycar CTBN 1300X13) produced by B.F. Goodrich Co.

Two types of epoxy resins were used for end-capping of CTBN oligomers. A polypropylene glycol diepoxide (DGEP) with an epoxy equivalent weight of about 340 g/eq, DER 732 resin from Dow Chemical Co., was employed as flexible end-capping agent. This is the same flexible end-capping agent em-

ployed by Chen and Jan.[20] A relatively low-molecular-weight DGEBA epoxy resin, DER 332 resin from Dow Chemical Co., with an epoxy equivalent weight of about 175 g/eq was used as rigid end-capping group. In summary, the DGEP-capped CTBN oligomer should develop an interphase with decreased crosslink density (more ductile) whereas the DGEBA-capped CTBN oligomer should develop an interphase with increased crosslink density (less ductile).

Processing

Curing of the epoxy was accomplished by the following procedure. First, the DDS and epoxy resin (9:1 amine–epoxy) were adducted at 180°C. The amine adduct was cooled down to room temperature. Then the rest of the epoxy required to maintain the stoichiometric amount of curing agent plus the appropriate amount of rubber–adduct were added. The mixture was reheated at about 140°C until complete melting followed by half an hour of mixing under vacuum to remove the entrapped air bubbles. Solution was then poured into a 6-mL-thick vertical aluminum mold which was preheated at 180°C. The materials were cured at 180°C for 2 h and then postcured for another 2 h at 220°C. In all formulations in this study 10 phr CTBN was employed. End-capping of CTBN was performed by prereacting of one-to-two molar ratio of liquid rubber to end-capping epoxy monomers. Prereacting was done at 150°C for 4 h under vacuum.

Characterization

A variety of characterization techniques were employed. Gel permeation chromatography (GPC) was used to ensure the proper preparation of CTBN adducts. Tensile and fracture toughness testing were employed to determine the material properties. Scanning electron and optical microscopy were used to elucidate the toughening mechanisms.

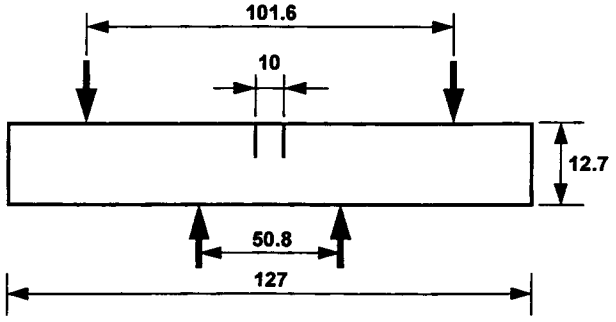

Figure 3 Schematic illustration of the double-notched four-point bending (DN-4PB) test geometry. Dimensions are in millimeters.

Table I Number-Average Molecular Weight (M_n) of Modifiers Used

Modifier	Expected (kg/mol)	Measured (kg/mol)
CTBN	3.1	3.0
CTBN–DGEBA	3.8	3.9
CTBN–DGEP	4.5	4.8

Number-average molecular weight (M_n) of CTBN and CTBN adducts made were measured using a Waters (type 201) GPC unit with a series of four ultastyragel columns with 10^2, 10^3, 10^4, 10^5 Å porosities. Dilute solutions (0.5%) in tetrahydrofuran (THF) were injected into the GPC. Flow rate of 1 mL/min was used in this study.

The tensile behavior of materials were evaluated in accordance with the ASTM D638 test method. Type I dogbone specimens were machined from the cured plaques. The specimens were tested using a screw-driven Instron testing frame at a crosshead speed of 5 mm/min. A clip-on extensometer was used to measure strain in the specimen gauge length. The results reported are averages of three tests.

Two types of specimens were used to determine fracture toughness (Fig. 2). Six-millimeter-thick samples were used for both types of specimens. The first test method employed precracked, single-edge notched (SEN) specimens loaded in three-point bending (3PB) geometry. The ASTM D5045 guideline was followed to measure the plane strain fracture toughness (K_{IC}) in this test. Precracks were introduced to the notched bars by hammering a razor blade which was chilled in liquid nitrogen. These tests were performed using a screw-driven Instron testing frame at a crosshead speed of 1 mm/min. K_{IC} values reported represent averages of a minimum of five tests. The following equations were used to calculate K_{IC}:

$$K_{IC} = \frac{10^{3/2} \times P \times S}{t \times w^{3/2}} f(X) \qquad (1)$$

and

$$f(X) = 3X^{1/2} \frac{1.99 - X(1-X)(2.15 - 3.93X + 2.7X^2)}{2(1+2X)(1-X)^{3/2}} \qquad (2)$$

Table II Tensile Properties of Modified Blends Containing 10 phr CTBN Rubber

Modifier	Yield Strength (MPa)	Elongation to Failure (%)	Modulus of Elasticity (GPa)
CTBN	71.5	4.5	2.70
CTBN-DGEBA	67.5	5.5	2.65
CBN-DGEP	66.0	7.5	2.70

where P is the critical load for crack propagation (kN), S is the span length (mm), t is specimen thickness (mm), w is specimen width (mm), $f(X)$ is a nondimensional shape factor, X is the crack length to specimen width ratio (a/w), and a is the crack length measured after the specimen breaks (mm).

The second test employed tapered double-cantilever beam (TDCB) specimens (Fig. 2). This type of specimen was employed to detect the contribution of crack wake mechanisms. Additionally, Chen and Jan[20] also used TDCB geometry for G_{IC} measurement in their study on the role of interphase ductility. G_{IC} values are calculated using the following equation:

$$G_{IC} = \frac{4P^2m}{Ebb'} \tag{3}$$

where P is load required to propagate the crack (N), m shape factor (0.496 mm^{-1} for the geometry seen in Fig. 2), E tensile modulus (MPa), b specimen width (mm), and b groove thickness (mm, $\sim 0.8b$). Similar precracking technique and loading conditions to that of SEN-3PB specimens were employed for TDCB samples.

Fracture surfaces of the SEN-3PB specimens were examined using a JEOL 6300F scanning electron microscope at an accelerating voltage of 5 kV. Samples were coated with a thin layer of gold-palladium before examination to protect the fracture surfaces from beam damage and also to prevent charge buildup.

Table III K_{IC} [a] of Modified Blends Containing 10 phr CTBN Rubber

Modifier	Fracture Toughness (MPa $m^{0.5}$)
CTBN	2.00
CTBN-DGEBA	2.00
CTBN-DGEP	1.90

[a] K_{IC} was determined using SEN samples in three-point bending.

In order to observe the crack tip damage zone of modified epoxies, double-notched four-point bending (DN-4PB) method in conjunction with transmission optical microscopy[21] was employed. Details of this technique are as follows:

First two edge cracks of equal length are introduced to a bending sample (Fig. 3). The specimen is then loaded in a four-point bending fixture until damage zones form at the crack tips. Finally, one of the cracks reaches the instability point and the sample fractures. The other crack which is unloaded, therefore, contains a well-developed damage zone that represents the conditions prior to the failure of the material. This damage zone can be observed using a transmission optical microscope after thinning via petrographic polishing.[21]

A screw-driven Instron testing frame at a crosshead speed of 1 mm/min was employed for breaking the samples. Thin specimens ($\sim 80\ \mu m$) taken from the midplanes of four-point bending samples were then viewed using an Olympus BH-2 microscope under crossed-polarized light.

RESULTS AND DISCUSSION

Materials

Number-average molecular weight (M_n) of modifiers used are shown in Table I. A modest difference between the expected and measured values of M_n, seen in this table, indicates that the CTBN adducts were successfully prepared. No particular characterization technique was employed in this study to detect the formation of an interphase around CTBN particles after curing of epoxy. However, based on the work of Sayer et al.,[22] one may expect an interphase around second-phase particles with a gradient of compositions of CTBN and epoxy matrix and also rich in end-capping molecules. Chen and Jan[20] were able to detect a diffuse interphase around their end-capped CTBN particles using transmission electron microscopy. The thickness of that interphase was about 150 nm, i.e., less than 10% of the size of their

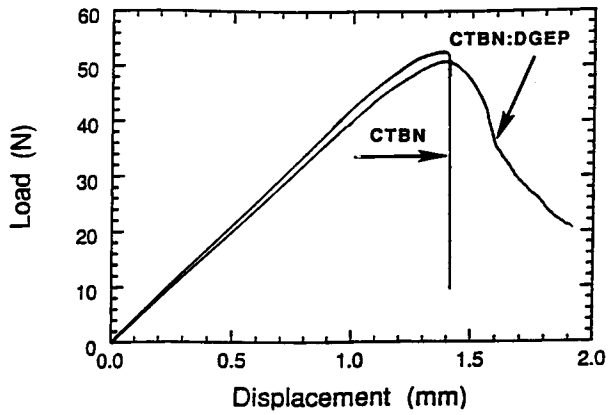

Figure 4 Load–displacement curves of two specimens tested in 3PB geometry for K_{IC} measurement. Legends on the figure specify the modifiers used.

original CTBN particles, when the rubber was end-capped with DGEP epoxy.[20]

Therefore, considering the GPC results, we may also expect to have an interphase surrounding our rubber particles when end-capped CTBN is used. The interphase would be stiff if the CTBN is end-capped with rigid DGEBA and ductile if flexible DGEP chains are employed. Formation of the interphase layer, as will be discussed later, is also inferred by differences observed in cavitation characteristics of particles.

Tensile Test and K_{IC} Measurement

The results of tensile tests are shown in Table II. As seen in Table II, yield strength of the blend was reduced by incorporation of either type of interphases. This observation could be explained by early cavitation of modified CTBN particles compared to the pure CTBN. It should be mentioned here that whitening of the tensile bars under loading conditions, which represents the cavitation of rubber particles, started at some point very close to the yield point in epoxy modified by pure CTBN. Whitening, however, started at much lower stresses in the other two cases. Since cavitation of rubber particles followed by dilation of the surrounding matrix increases the actual volume fraction of the holes, one would expect lower yield strength in cases where particles cavitate earlier. Indeed, the recent work by Dijkstra et al.[23] on rubber-modified nylon revealed that the yield stress of the blend would decrease if particles with lower cavitation resistance are employed. However, it should be mentioned that our own work on epoxies modified with hollow plastic spheres illustrates that this concept may not hold for submicron particles.[24] Since, the particles here are greater than 1 μm then one would expect the yield stress to drop if the particles cavitate prior to the yield point.

Elongation to failure was improved by introduction of both interphases (Table II). This improvement was, however, much more pronounced in the case of CTBN–DGEP-modified epoxy. One possible rationale for this observation could be the suppres-

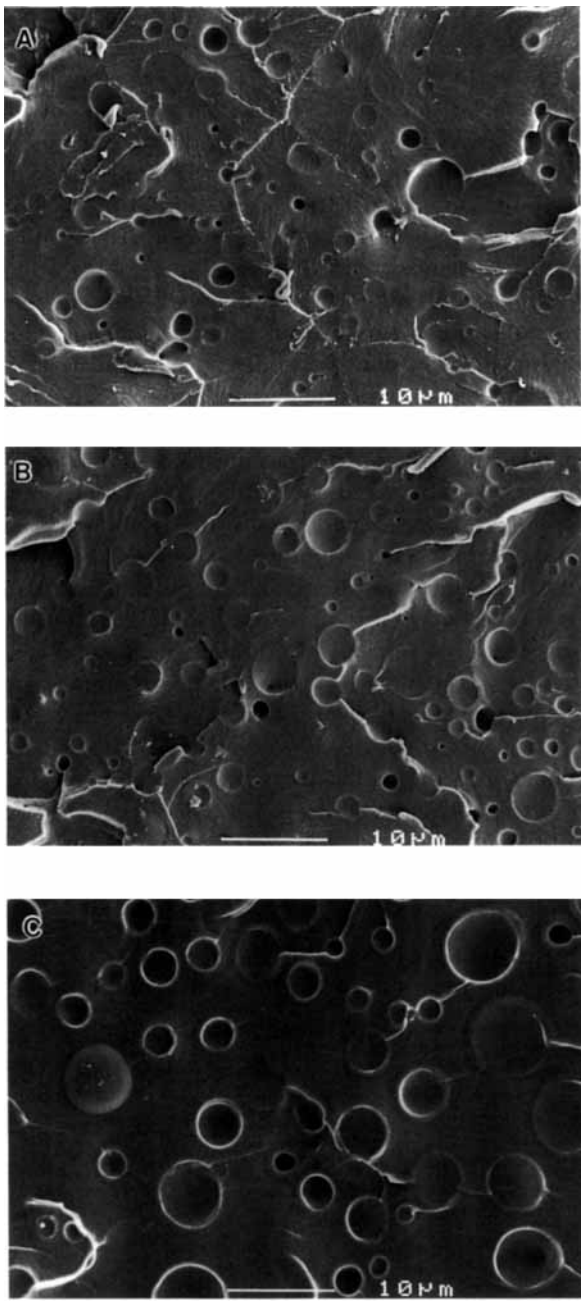

Figure 5 SEM micrographs taken from the fast fracture region of SEN-3PB samples of epoxies modified by (a) CTBN, (b) CTBN–DGEBA, and (c) CTBN–DGEP.

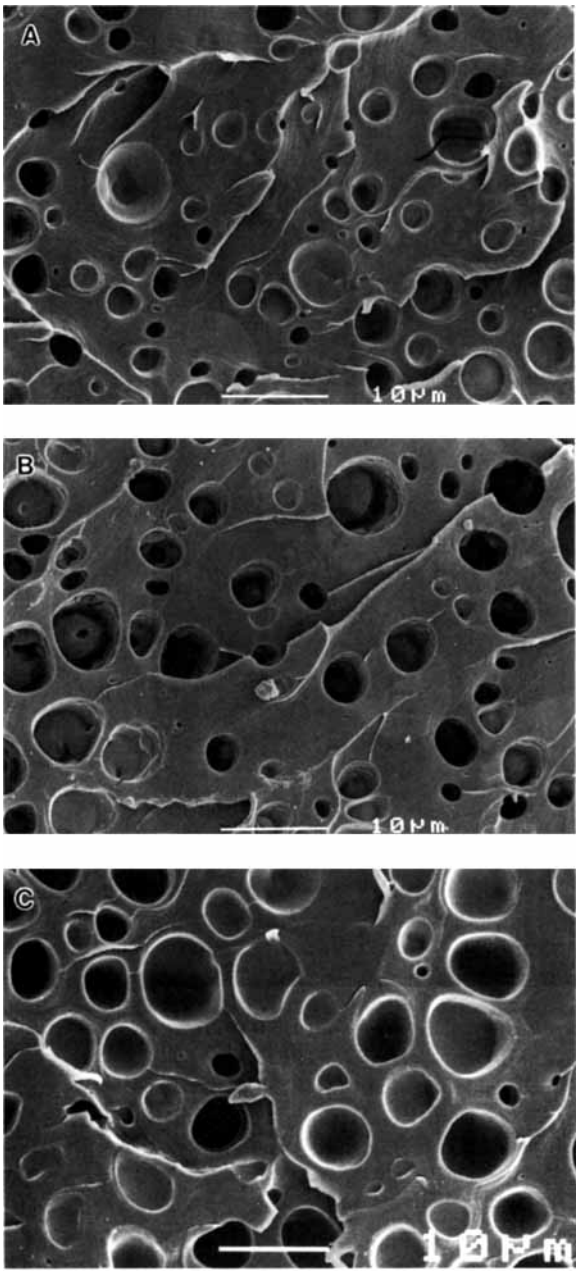

Figure 6 SEM micrographs taken from the damage zone of SEN-3PB samples of epoxies modified by (a) CTBN, (b) CTBN–DGEBA, and (c) CTBN–DGEP.

sion of cracking at the matrix adjacent to rubber particles due to the presence of the ductile interphase. Please note that in tensile test the sample is assumed to be flaw free, however, the rubber particles can act as stress concentrators or internal flaws that initiate cracks in the neighboring matrix. Consequently, the presence of a ductile shell around the particles may postpone the crack initiation in those areas. No considerable difference among the moduli of elasticity was found (Table II). This is because the slope of stress–strain curves at early stages of loading were used for moduli calculation and no cavitation has occurred in that loading range.

Based on the tensile data, one expects to see the maximum toughness in the case of epoxy modified with CTBN–DGEP, since this material has the largest area under the stress–strain curve and the lowest yield stress. Please note that the area underneath the stress–strain curve in tension is traditionally considered as a measure of toughness. The result of K_{IC} measurement, however, disagrees with this hypothesis and shows an almost identical fracture toughness in all three cases (Table III). This observation could be explained considering the fact that cracked specimens are used for K_{IC} measurement. In other words, contrary to that of tensile test, suppression of cracking in the matrix adjacent to rubber particles is not an important issue in this case since the flaw already exists in the sample.

Despite identical fracture toughness values (Table III), the material modified with CTBN–DGEP displayed a different type of crack growth behavior. Figure 4 shows the load–displacement curves of two SEN-3PB samples with the same dimensions and crack lengths. As seen in this figure, the maximum load used for K_{IC} calculation is nearly the same for two samples leading to the similar K_{IC} values. The material modified with CTBN–DGEP, however, tends to resist against crack growth after peak load where the crack grows slowly. CTBN-modified material, on the other hand, shows a fast fracture behavior at the peak load (Fig. 4). This behavior against crack growth, which occurred in all samples, indicates that there is a potential for improved toughening in CTBN–DGEP-modified material. This potential, however, is not strong enough to improve the fracture toughness of the material in the conventional method for determining fracture toughness. One may argue that the difference in crack growth behavior seen in Figure 4 could disappear at higher strain rates. While we do not disagree with this idea, we believe that Figure 4 illustrates a real difference between the crack growth behavior of these materials at the present test conditions.

Scanning Electron Microscopy (SEM)

Figure 5 contains the SEM micrographs taken from the fast fracture region of SEN-3PB specimens. Since plastic dilation of the epoxy matrix does not occur in this zone, micrographs taken from this region represent the original size of the rubber par-

ticles. Figure 6 contains similar SEM micrographs to that of Figure 5, but taken from the damage zone. Comparing the average size of the particles in the fast fracture region (Fig. 5) with that of the damage zone (Fig. 6), one finds the degree of dilation of particles.[20] Original size of the rubber particles, their average size after dilation, and the degree of dilation are shown in Table IV.

Variation of particle size with introducing the end-capping groups (Fig. 5) could be explained primarily by means of difference in solubility parameter, viscosity, and surface tension of the rubbery phase and to a lesser extent in molecular weight of the original rubber.[22] Regardless of differences in size of the original particles, Table IV clearly shows a difference in dilatation around the different types of CTBN adducts used, which could be attributed to the presence of the interphases. Introduction of the rigid interphase, as seen in Figure 6, was associated with ease of debonding at the particle–matrix interface. Ease of debonding in this case is attributed to a reduction of interfacial strength between CTBN and epoxy. The ease of debonding may be responsible for extra dilatation in this material compared to that of epoxy modified with pure CTBN.

Having a higher degree of dilation in material modified by CTBN–DGEP compared to that of CTBN (Table IV) is consistent with what Chen and Jan[20] found for a DGEBA/piperidine-cured epoxy. These researchers attributed this observation to the ease of void growth when the rubber particle is embedded in a ductile surrounding. The same researchers, in another study,[25] investigated the effect of the size of such a ductile surrounding by end-capping their CTBN rubber with DGEP epoxies with different molecular weight. They found an increase in thickness of the interphase, a higher degree of dilation, and a higher fracture energy when CTBN was end-capped with longer epoxy chains. These researchers, thus, concluded that a thicker interphase allows the matrix surrounding the rubber particles to dilate to a higher extent and therefore, dissipates more energy.[25]

Figure 6 does not show any sign of debonding around CTBN–DGEP particles. Therefore, we may borrow the same rationale that Chen and Jan[20,25] proposed for increased dilation when ductile interphases are surrounding the rubber particles. Our K_{IC} measurement (Table III), however, illustrates no benefit of extra dilatation in fracture toughness improvement, meaning that additional dilation or void growth does not necessarily improve fracture toughness.

Transmission Optical Microscopy (TOM)

Figure 7 illustrates the plastic zone of modified epoxies viewed using TOM. Plastic zone and cavitation zone sizes are reported in Table V. Predicted plastic zone sizes in this table are calculated using the Irwin equation[26]:

$$2r_y = \frac{2}{6\pi}\left(\frac{K_{IC}}{\sigma_y}\right)^2 \tag{4}$$

where $2r_y$ is the plane strain plastic zone size and σ_y is the yield stress of material. Real plastic zone sizes, however, are obtained by measuring the height of the damage zones in Figure 6. Cavitation zone sizes are obtained by measuring the diameter of the stress-whitened zones of the DN-4PB samples.

Increase in cavitation zone size (Table V) and observation of higher degree of dilation in CTBN adducts (Table IV) represent that end-capping of CTBN rubber reduces the cavitation resistance of the second-phase particles. Early signs of stress whitening seen in tensile tests also indicate the lower cavitation resistance of these particles compare to that of pure CTBN particles.

The significant enlargement of the plastic zone by introduction of the rigid shell compared to that of pure CTBN (Fig. 7) could be attributed to the particle size effect. Note that the introduction of rigid shell to CTBN rubber resulted in an increase in average particle size from 2.0 to 2.7 μm (Table IV). Since these materials have the same K_{IC}, it seems reasonable that larger particles yield a more feathery and less dense, and thus, larger plastic zone size. In case of CTBN–DGEP-modified material, the

Table IV Average Size of Rubber Particles and Degree of Matrix Dilation

Modifier	Before Dilation (μm)	After Dilation (μm)	Degree of Dilation (%)
CTBN	2.0	2.6	30
CTBN–DGEBA	2.7	4.2	55
CTBN–DGEP	3.5	5.4	54

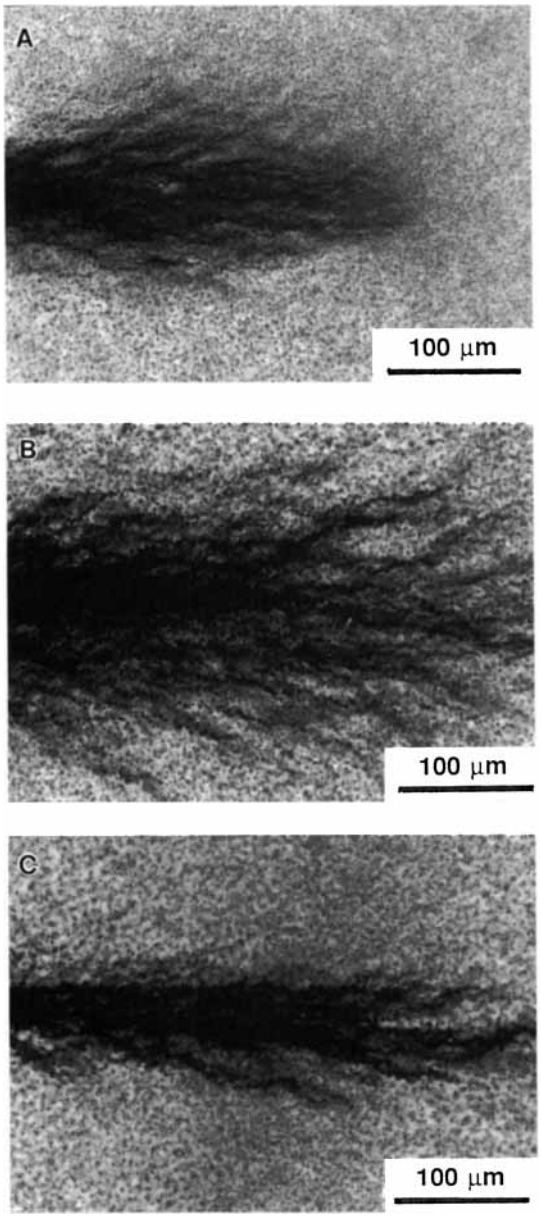

Figure 7 TOM micrographs taken from the midplane of the crack tip damage zone in epoxies modified by (a) CTBN, (b) CTBN–DGEBA, and (c) CTBN–DGEP.

plastic zone is even smaller than that of the pure CTBN (Table V). The shape of the plastic zone in this case is also different from those of CTBN and CTBN–DGEBA-modified epoxies (Fig. 7). Having almost the same K_{IC} but different plastic zone size and shape compared to the other two materials indicates a possible difference in toughening mechanism occurring in the CTBN–DGEP-modified material. Slow crack growth behavior in this material after peak load in K_{IC} test (Fig. 4) could be also related to the same mechanism.

Toughening Mechanism

In order to elucidate the exact toughening mechanism in epoxy modified by CTBN–DGEP, a closer examination of fracture surfaces was conducted. Figure 8 illustrates the SEM micrographs of damage zone of the three materials used at higher magnification than that of Figure 6. As seen in this figure, in case of ductile shell (CTBN–DGEP-modified material), a pronounced ridge is seen around every particle. Formation of these ridges cannot be simply attributed to the increased dilation of particles. Please note that the same degree of dilation was found for CTBN–DGEBA particles (Table IV), while ridges are not seen around these particles [Fig. 8(b)]. Ridges seen in Figure 8(c), if viewed at some angle to the loading direction (Fig. 9), are actually highly stretched materials around the particles. The presence of these stretched ridges around CTBN–DGEP particles suggest a form of matrix–interphase bridging occurred in this system. This concept is schematically shown in Fig. 10.

Consequently, it could be hypothesized that end-capping of CTBN rubber by flexible epoxy chains results in formation of ductile interphases around particles. These interphases then act as tiny bridges and resist against crack growth since they are more deformable than the matrix and can tolerate higher extensions. The traction forces supplied by interphase bridges may also reduce the applied K and thus contribute to the overall fracture toughness. Since the epoxy modified by CTBN–DGEP particles has the same K_{IC} that other materials have (Table III), occurrence of bridging mechanism in this material should result in formation of a smaller plastic zone size compared to the other two materials. This fact is evidenced in Figure 7 where plastic zone size of the modified epoxies are shown.

Since the size of interfacial bridges scale with the size of rubber particles, it is reasonable to have a very small bridging zone when using a low-compliant specimen like SEN-3PB. This is probably why formation of these bridges have a modest effect in 3PB tests, i.e., suppression of fast fracture, and do not contribute in K_{IC} improvement (Fig. 4). This hypothesis implies that having a more compliant sample, such as tapered double-cantilever beam, where a larger bridging zone can be developed, would result in increased toughness.

Tapered Double-Cantilever Beam (TDCB) Test

The results of G_{IC} measurement using the TDCB technique are shown in Table VI, which illustrate

Table V Plastic Zone and Cavitation Zone Sizes Measured in Modified Epoxies

Material	Predicted Plastic Zone Size[a] (μm)	Measured Plastic Zone Size[b] (μm)	Measured Cavitation Zone Size[c] (μm)
CTBN	83	133	1100
CTBN–DGEBA	93	200	4800
CTBN–DGEP	88	111	4300

[a] Plane strain plastic zone size calculated using Eq. four.
[b] The height of plastic zones measured in Figure 6.
[c] The diameter of whitened zone at the crack tip in DN-4PB samples.

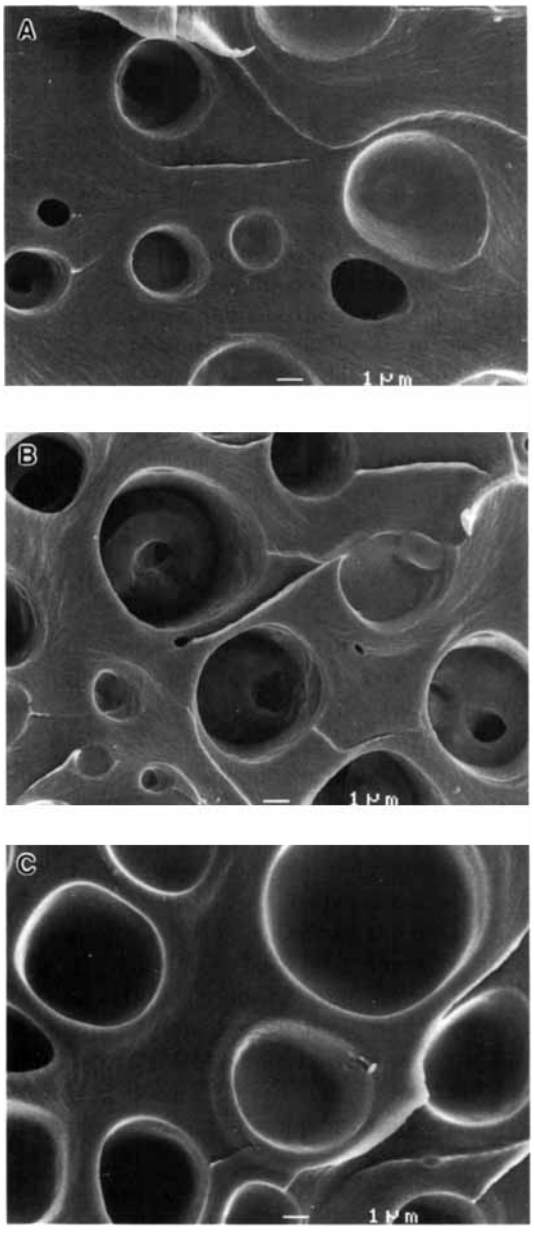

Figure 8 Same as Figure 6, but at higher magnification.

the superiority of the ductile shell in toughness improvement. Comparing these results with that of K_{IC} measurement using SEN-3PB shown in Table III, one realizes that the advantage of the ductile interphase is dependent on the type of test method. In other words, use of TDCB in place of 3PB geometry, which magnifies the influence of crack wake mechanism(s), reveals an improvement in fracture toughness by modification of interphase. This finding reinforces the aforementioned hypothesis on bridging of ductile interphases, meaning that one can benefit from bridging of deformable interphases around rubber particles if it generates a large enough bridging zone that allows a significant amount of

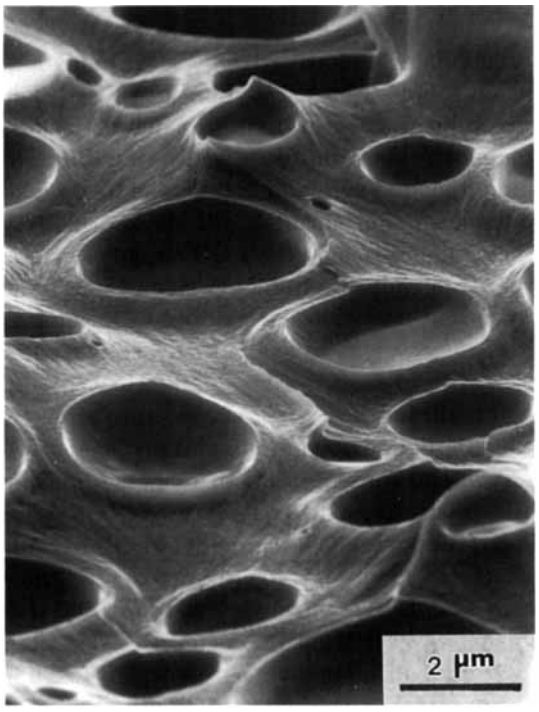

Figure 9 SEM micrograph of epoxy modified by CTBN–DGEP viewed at 60° to the loading direction.

tiny bridges, which contribute in crack growth resistance.

This study does not refute the notion that interphase modification can lead to improved toughness. However, it does refute the hypothesis of Chen and Jan[20,25] that the introduction of ductile interphase around CTBN particles enhances fracture energy by promoting dilation of epoxy matrix around the rubber particles. Instead, we propose that the occurrence of interfacial bridges can contribute significantly to improve fracture toughness, albeit under certain test conditions. Improvement in crack growth resistance by introduction of such an interphase is only observed when a compliant specimen such as TDCB is used.

CONCLUSIONS

Rigid and ductile interphases were introduced to rubber particles in a DGEBA epoxy matrix by prereacting the CTBN rubber with different epoxy monomers. Mechanical performance of the materials were characterized via several techniques. The following conclusions were made:

1. End-capping of CTBN oligomers with either rigid or flexible epoxy chains enlarges the size of rubbery precipitates and also promotes dilatation of the matrix surrounding the particles. Debonding at the interface, in case of the rigid shell, and plasticity of the surrounding medium, in case of ductile interphase, appear to be responsible for the increase in degree of dilation.
2. Introduction of the ductile shell enhances elongation to failure in tensile test significantly. Suppression of crack initiation in the adjacent matrix by deformable interphase may contribute to this observation.
3. Presence of ductile interphase around CTBN particles tends to stabilize cracking at triaxial stress field of the crack tip via formation of tiny interphase bridges around CTBN particles.
4. Interfacial bridging was found to be beneficial if a large number of bridges are involved, i.e., fracture specimen should have a relatively large crack length–crack opening ratio.

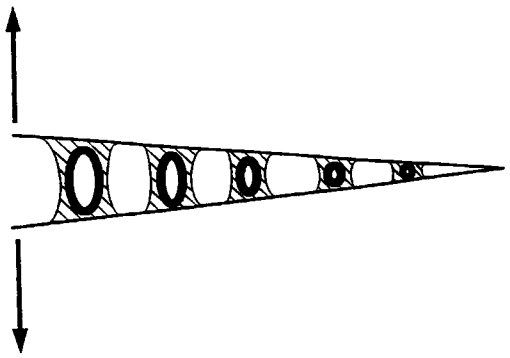

Figure 10 Schematic showing the bridging of deformable interphases that tend to stabilize the crack growth.

Table VI G_{IC} [a] of Modified Blends Containing 10 phr CTBN Rubber

Modifier	Fracture Energy (kJ/m^2)
CTBN	1.95
CTBN-DGEBA	1.90
CTBN-DGEP	2.65

[a] G_{IC} was determined using TDCB method.

The authors would like to acknowledge the financial support provided by Polymer Interfaces Center of Lehigh University and National Science Foundation (Grant Nos. MSS-9211664 and ECD-9117064).

REFERENCES

1. J. N. Sultan, R. C. Liable, and F. J. McGarry, *Polym. Symp.*, **16,** 127 (1971).
2. J. N. Sultan and F. J. McGarry, *Polym. Eng. Sci.*, **13,** 29 (1973).
3. W. D. Bascom, R. L. Cottington, R. L. Jones, and P. Peyser, *J. Appl. Polym. Sci.*, **19,** 2425 (1975).
4. C. K. Riew, E. H. Rowe, and A. R. Siebert, *ACS Adv. Chem. Ser.*, **154,** 326 (1976).
5. S. Kunz-Douglass, P. W. R. Beaumont, and M. F. Ashby, *J. Mater. Sci.*, **15,** 1109 (1980).
6. J. A. Sayer, S. C. Kunz, and R. A. Assink, *ACS Div. Polym. Mater. Sci. Eng.*, **49,** 442 (1983).
7. A. J. Kinloch, S. J. Shaw, D. A. Tod, and D. L. Hunston, *Polymer*, **24,** 1355 (1983).
8. A. F. Yee and R. A. Pearson, *J. Mater. Sci.*, **21,** 2462 (1986).
9. A. J. Kinloch, C. A. Finch, and S. Hashemi, *Polym. Commun.*, **28,** 322 (1987).
10. R. A. Pearson and A. F. Yee, *J. Mater. Sci.*, **24,** 2571 (1989).
11. R. A. Pearson and A. F. Yee, *J. Mater. Sci.*, **26,** 3828 (1991).
12. Y. Huang and A. J. Kinloch, *J. Mater. Sci.*, **27,** 2763 (1992).

13. Y. Huang and A. J. Kinloch, *J. Mater. Sci. Lett.*, **11,** 484 (1992).
14. V. V. Kozii and B. A. Rozenberg, *Polym. Sci.*, **34,** 919 (1992).
15. C. K. Riew, E. H. Rowe, and A. R. Siebert, *Advances in Chemistry Series,* No. 154, R. D. Deanin and A. M. Crugnola, Eds., ACS, Washington, D.C., 1976, p. 326.
16. L. Chan, J. K. Gillham, A. J. Kinloch, and S. J. Shaw, *Advances in Chemistry Series,* No. 208, C. K. Riew and J. K. Gillham, Eds., ACS, Washington, D.C., 1984, p. 261.
17. Y. Huang, A. J. Kinloch, R. Bertsch, and A. R. Sibert, *Advances in Chemistry Series,* No. 233, C. K. Riew and A. J. Kinloch, Eds., ACS, Washington, D.C., 1993, p. 189.
18. R. Bagheri and R. A. Pearson, *9th Int. Conf. Deformation, Yield, and Fracture of Polymers,* Cambridge, UK, 1994, p. 106.
19. V. A. Matonis, *Polym. Eng. Sci.*, **9,** 100 (1969).
20. T. K. Chen and Y. H. Jan, *Polym. Eng. Sci.*, **31,** 577 (1991).
21. H. J. Sue, R. A. Pearson, D. S. Parker, J. Huang, and A. F. Yee, *ACS Div. Polym. Chem., Polym. Prep.*, **29,** 147 (1988).
22. J. A. Sayre, R. A. Assink, and R. R. Lagasse, *Polymer,* **22,** 87 (1981).
23. K. Dijkstra, A. van der Wal, and R. J. Gaymans, *J. Mater. Sci.*, **29,** 3489 (1994).
24. R. Bagheri and R. A. Pearson, unpublished reports.
25. T. K. Chen and Y. H. Jan, *J. Mater. Sci.*, **26,** 5848 (1991).
26. G. R. Irwin, *J. Appl. Mech.*, **24,** 361 (1957).

Received November 1, 1994
Accepted February 14, 1995